Determination of Sensitizer Regeneration Efficiency in Dye-Sensitized Solar Cells

Feng Li,[†] James Robert Jennings,[†] and Qing Wang*

Department of Materials Science and Engineering, Faculty of Engineering, NUSNNI-NanoCore, National University of Singapore, Singapore 117576. [†]F. Li and J. R. Jennings contributed equally.

ABSTRACT Regeneration of the sensitizing dye in dye-sensitized solar cells (DSCs) is frequently studied using the transient absorption (TA) technique. However, TA measurements are generally not performed using complete DSCs at the maximum power point (MPP) on the current—voltage (*j*—*V*) characteristic, and the electron concentration in the nanocrystalline TiO_2 films used in these devices is often not well characterized, which may lead to results that are not relevant to actual solar cell operation. Here, dye regeneration kinetics were studied at the MPP and at open circuit (where interpretation of results is simpler) in DSCs employing a "robust" nonvolatile 3-methoxypropionitrile-based electrolyte solution. Using a combination of TA, differential incident photon-to-current efficiency measurements, and impedance spectroscopy, the dependence of electron—dye recombination rate and overall sensitizer regeneration efficiency on TiO_2 electron concentration is unambiguously demonstrated. We also examine the validity of a commonly used approach for determining regeneration efficiency in which the electron—dye recombination rate constant is estimated from TA decays of cells employing a redox-inactive electrolyte solution. We find evidence that this widespread practice may be unsuitable for accurate determination of the regeneration rate constant or efficiency. We go on to show that, despite near-quantitative regeneration at short circuit or low photovoltage, power conversion efficiency is limited by inefficient regeneration in stable DSCs with practically relevant electrolyte solutions.

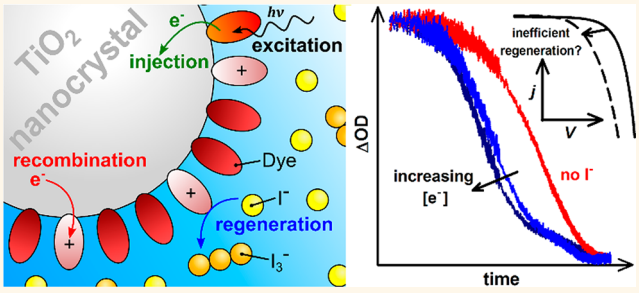

KEYWORDS: dye-sensitized solar cells · regeneration · recombination · transient absorption · incident photon-to-current efficiency · impedance spectroscopy · working conditions

Power conversion efficiencies (PCEs) in excess of 12%[1] and potentially low manufacturing costs make dye-sensitized solar cells (DSCs)[2] a serious competitor to conventional silicon-based photovoltaics. At the heart of the DSC is a monolayer of dye molecules (D) adsorbed on a wide band gap semiconductor, such as TiO_2, that harvests sunlight by absorbing incident photons. Following light absorption, excited dye molecules (D*) inject electrons into the semiconductor (e^-), themselves becoming oxidized in the process (D^+).

$$D + h\nu \rightarrow D^* \quad \text{(R1)}$$

$$D^* \rightarrow D^+ + e^- \quad \text{(R2)}$$

As a regenerative-type photoelectrochemical cell,[3] the oxidized dye is then rereduced, or "regenerated", by the reduced half of a redox couple in the electrolyte solution. Although the regeneration process is critical to DSC operation, *in situ* studies of regeneration in complete, operational DSCs are relatively rare compared to studies of electron transport or recombination of TiO_2 electrons with acceptors in the electrolyte solution. This may be partly due to several early studies of DSCs[4−8] that found evidence for efficient regeneration. The assumption of efficient regeneration then became relatively common in much of the work focused on characterization and modeling of DSCs. Recently, however, a few authors have revisited the problem of regeneration in functional DSCs under more operationally relevant conditions, and the need for more accurate measurements of regeneration in complete devices has been pointed out.[9−11]

One of the most successful redox couples in DSCs is I_3^-/I, which is thought to regenerate ruthenium bipyridyl dyes by these

* Address correspondence to qing.wang@nus.edu.sg.

Received for review July 18, 2013 and accepted August 13, 2013.

Published online August 13, 2013
10.1021/nn403714s

three steps:[9,12−15]

$$D^+ + I^- \rightarrow (D^+ \cdots I^-) \quad \text{(R3)}$$

$$(D^+ \cdots I^-) + I^- \rightarrow D + I_2^{-\bullet} \quad \text{(R4)}$$

$$2I_2^{-\bullet} \rightarrow I^- + I_3^- \quad \text{(R5)}$$

First, D^+ reacts with I^- forming the complex $(D^+ \cdots I^-)$; then with the approach of a second I^- ion charge transfer is completed and the complex dissociates, yielding D and $I_2^{-\bullet}$. $I_2^{-\bullet}$ radicals subsequently disproportionate to produce I_3^- and I^-. Step R3 is rate-limiting, and the overall reaction is thus first order in [I−]. In contrast, recent work shows that regeneration of some organic dyes is second order in [I^-], pointing to R4 being rate limiting.[16]

Competing with the regeneration process is the undesirable recombination of e^- with D^+, termed electron−dye recombination (EDR).

$$D^+ + e^- \rightarrow D \quad \text{(R6)}$$

The overall efficiency of regeneration can be derived from the continuity equation for D^+ and, for regeneration that is first order in [I^-] as for standard ruthenium dyes, can be expressed as

$$\eta_{rg} = \frac{k_{rg}[I^-]}{k_{obs,\,D^+}} = 1 - \frac{k_{edr} n_{tot}^{\chi}}{k_{obs,\,D^+}} \quad (1)$$

where $k_{obs,D+}$ is the observed pseudo-first-order rate constant for the decay of D^+:

$$k_{obs,\,D^+} = k_{rg}[I^-] + k_{edr} n_{tot}^{\chi} \quad (2)$$

k_{rg} and k_{edr} are the rate constants for dye regeneration by I^- and EDR, respectively, n_{tot} is the total electron concentration in the TiO_2, and χ is the EDR reaction order in n_{tot}.

Dye regeneration efficiency is directly proportional to the photocurrent of the cell and is a prerequisite for any efficient DSC. Near-unity regeneration efficiencies have been inferred from TA measurements for a variety of different redox couples under what are essentially open-circuit conditions, although generally not using realistic electrolyte solutions and a well-defined background electron concentration in the TiO_2.[17−20] In most studies, sensitized TiO_2 films immersed in electrolyte solution were characterized instead of real devices under working conditions, which could lead to irrelevant results. As indicated by eq 1, EDR may compete with regeneration under conditions with relatively high n_{tot},[11,21,22] such as at the maximum power point (MPP) on the j−V curve. Although evidence for accelerated EDR under operating conditions has been found in numerical simulations and indirect photoelectrochemical studies,[10,11] and EDR has been observed in redox-inactive electrolyte solutions using transient absorption (TA) measurements,[8,23] no direct evidence from TA for reduced regeneration efficiency at the MPP has been reported. Since efficient regeneration is critical for device functioning, it is important to perform TA experiments at the MPP, where EDR may not be negligible. It is also important to more accurately characterize and control the electron concentration in the TiO_2 film during measurements, rather than simply adjusting the laser pulse energy to inject approximately "one electron per particle". With this in mind, we have used TA in conjunction with differential incident photon-to-current efficiency (IPCE) measurements and impedance spectroscopy (IS) to investigate regeneration and recombination kinetics in DSCs at the MPP and under open-circuit conditions, where interpretation of measurements is simpler. The validity of the model used is examined in detail by various comparisons between steady-state and dynamic measurements. We have also examined electron−dye recombination kinetics in cells with redox-inactive "inert" electrolyte solutions in order to determine whether kinetic parameters derived from such samples are suitable for calculating the regeneration efficiency in DSCs with full, redox-active electrolyte solutions.

RESULTS AND DISCUSSION

Determination of Dye Regeneration Efficiency Using Transient and Steady-State Approaches. The DSCs studied here are based on a 3-methoxypropionitrile I_3^-/I^- electrolyte solution and the Z907 sensitizer, a system that is known to be stable and reasonably efficient.[24] This choice of cell configuration helps ensure stability during extended measurements and is also partly driven by the desire to improve the PCE of stable DSCs,[24,25] which lags behind that of champion cells. EDR was also studied in the absence of competing dye regeneration by I^- using cells with an inert electrolyte solution (without I^- or I_2). In these cells the I^- salt was replaced with an ionic liquid (1-ethyl-3-methylimidazolium bis(trifluoromethylsulfonyl)-imide) to maintain the same ionic strength as the regular electrolyte solution. Full experimental details are given in the Methods section at the end of the article.

For the measurement and interpretation of TA data, a protocol similar to that established by Anderson *et al.* was adopted.[9] A sum of two stretched exponential functions was used to fit the decay of the laser-induced change in optical density (ΔOD) recorded at 830 nm, where both oxidized dye and TiO_2 electrons absorb (the known absorption of $I_2^{-\bullet}$ at this wavelength was assumed to track the D^+ absorption and so was not considered separately).[9,26]

$$\Delta OD_{830}(t) = \Delta OD_{0,\,D^+} \exp\left[-\left(\frac{t}{\tau_{WW,\,D^+}}\right)^{\beta_{D^+}}\right] + \Delta OD_{0,\,e^-} \exp\left[-\left(\frac{t}{\tau_{WW,\,e^-}}\right)^{\beta_{e^-}}\right] \quad (3)$$

For data recorded at 980 nm, where D^+ does not absorb, only one stretched exponential was used.

$$\Delta OD_{980}(t) = \Delta OD_{0,e^-} \exp\left[-\left(\frac{t}{\tau_{WW,e^-}}\right)^{\beta_{e^-}}\right] \quad (4)$$

In these expressions, ΔOD_0 is the initial laser-induced change in the optical density of the sample, τ_{WW} is the characteristic stretched exponential lifetime, β is the stretch parameter, and the subscripts D^+ and e^- denote parameters describing the decay of these species. As direct comparison of τ_{WW} values could be meaningless if β varies, weighted average lifetimes (τ_{obs}) were calculated using

$$\tau_{obs} = \frac{1}{k_{obs}} = \frac{\tau_{WW}}{\beta}\Gamma\left(\frac{1}{\beta}\right) \quad (5)$$

where $\Gamma()$ is the gamma function. Weighted-average lifetimes are appropriate for calculating concentrations and fluxes of species under steady-state conditions and can be used in the calculation of the steady-state regeneration efficiency (eq 1). By fitting the TA decays of regular cells (*i.e.*, with the full electrolyte solution containing I^-), k_{obs} for the D^+ and e^- decays (k_{obs,D^+} and k_{obs,e^-}) were calculated from the τ_{WW} and β values obtained from measurements made over a range of background illumination intensities. Assuming that the measurements are made in the small-perturbation regime, k_{obs,D^+} can be interpreted with eq 2, while $k_{obs,e^-} = \gamma k'_{eer} n_{tot}^{\gamma-1} + \chi k_{edr} n_{tot}^{\chi-1}[D^+]_{bg}$ where γ and k'_{eer} are the reaction order in n_{tot} and rate constant, respectively, for recombination of electrons with acceptors in the electrolyte solution (termed EER) and $[D^+]_{bg}$ is the background D^+ concentration.

Figure 1 shows a representative example of the measured 830 nm TA decays at various open-circuit photovoltages (for clarity only data for one cell are shown). Note that as the photovoltage increases the traces gradually shift to shorter times, indicating increasing k_{obs,D^+}. Initially, TA decays with 980 nm probe light were also recorded and fitted with eq 4 in order to fit the 830 nm TA with eq 3 while fixing all three parameters in the second term (assuming the absorption coefficients of electrons at 830 and 980 nm are the same); however, the resultant fitting quality was not always satisfactory. Fortunately, we find that there is sufficient detail in the TA decays at high voltage (*e.g.*, 769 mV) to fit for all six parameters in eq 3, with standard errors in the parameter estimates all being ≤0.85%. For measurements at lower voltages (*e.g.*, 610 mV), separation of the two decays is more difficult. Therefore, to fit the low voltage TA it was first assumed that the injection efficiency is constant in the voltage range studied here (this assumption is supported by the nearly identical ΔOD values at $t = 0$ s, which show no voltage-dependence). Justified by this assumption, the ratio of $\Delta OD_{0,D^+}/\Delta OD_{0,e^-}$ for low voltage TA was

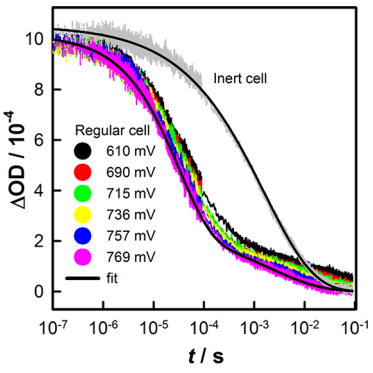

Figure 1. Measured transient absorption (TA) at 830 nm for a regular cell (redox-active electrolyte solution containing I^-) at various open-circuit photovoltages. The TA decay for an inert cell (no I^- or I_2 in the electrolyte solution) measured without background illumination is also shown for comparison. The black lines are representative single or double stretched exponential fits to the data.

fixed based on the fitting results for higher voltage TA, thus reducing the number of free parameters from 6 to 5. Using this procedure the remaining free parameters could be obtained, with standard errors in all parameters of ≤0.5%. In further support of the validity of the six parameter fits, we also find that k_{obs,e^-} values obtained from fits to 830 nm decays agree reasonably well with those obtained from three-parameter fits to 980 nm decays (Supporting Information).

TA decays for inert cells (without I^- and I_2) were also measured using an identical laser pulse energy but without background illumination. Experiments like this are commonly used to estimate the EDR rate constant so that the regeneration rate constant and regeneration efficiency can be calculated for regular cells using eq 1 and eq 2. Representative data and a fit are shown in Figure 1. The D^+ decay is clearly much faster in the regular cells containing I^- than in the inert cell, which intuitively suggests efficient dye regeneration. However, there are a number of reasons that the EDR rate constant estimated from inert cells may not be strictly applicable to regular cells, as we will discuss in detail later in this article. In order to calculate η_{rg} in the absence of separate measurement of $k_{edr}n_{tot}^{\chi}$, $k_{rg}[I^-]$ has been extracted by fitting eq 2 to $k_{obs,D}{}^+$ as a function of n_{tot} with the assumption of constant $k_{rg}[I^-]$, as shown in Figure 2. Here, n_{tot} is taken to be the background electron concentration in the cell either before (n_{bg}) or immediately after (n_{peak}) the laser excitation and is determined by integration of the TiO_2 capacitance (C_μ) obtained from IS measurements using

$$n_{tot} = \frac{1}{dAq}\int_0^{V_{oc}} C_\mu(V)\, dV \quad (6)$$

where d is the film thickness, A is the cell area, q is the elementary charge, and V_{oc} is either the open-circuit voltage before laser excitation (V_{bg}) or the voltage peak that shortly follows the laser pulse (V_{peak}), giving rise to

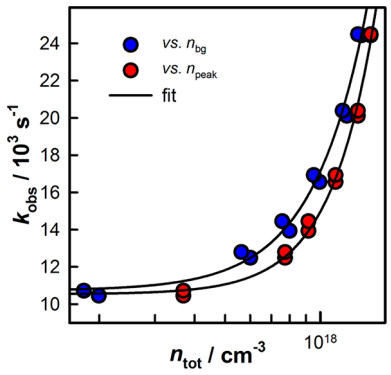

Figure 2. Dependence of the observed rate constant for the decay of the oxidized dye (k_{obs}) on TiO_2 electron concentration (n_{bg} or n_{peak}, see main text for definition) obtained from transient absorption measurements made at 830 nm on regular cells (data for two cells are shown in each plot) with a redox-active electrolyte solution. The line is a fit of eq 2 to the data, from which the electron−dye recombination rate constant, reaction order in n_{tot}, and regeneration rate constant can be determined.

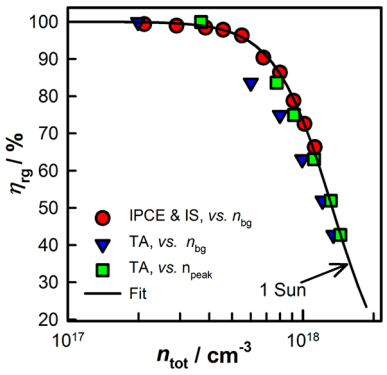

Figure 3. Dye regeneration efficiency (η_{rg}) calculated using the methods described in the main text, as a function of TiO_2 electron concentration (n_{tot}). Note the similarity between the plots obtained from transient absorption (TA) measurements and differential incident photon-to-current efficiency (IPCE) measurements combined with impedance spectroscopy (IS). The black line is a fit of eq 1 to the η_{rg} data derived from IPCE/IS measurements.

the two different electron concentrations, n_{bg} and n_{peak}, which will be discussed in more detail later.

The fit of eq 2 to the data is good, and approximate standard errors in $k_{rg}[I^-]$ and χ are quite small, with parameter estimates of (1.05 ± 0.03) × 10^4 s^{-1} and 3.07 ± 0.19, respectively, from the n_{peak}−k_{obs} plot or (1.08 ± 0.04) × 10^4 s^{-1} and 2.54 ± 0.25 from the n_{bg}−k_{obs} plot. On the other hand, the estimates for k_{edr} appear to be very inaccurate (*e.g.*, (2.7 ± 21.7) × 10^{-52} $cm^{3\chi}$ s^{-1} for the n_{peak}−k_{obs} plot). This is not surprising, as k_{edr} is sensitive to n_{tot}^{χ} where n_{tot} is very large (10^{17} to 10^{18} cm^{-3} in our data set) and χ is substantially larger than unity; thus a small error in the determination of n_{tot} and/or χ will lead to a very large error in k_{edr}. However, the fact that the approximate 95% confidence interval for k_{edr} contains zero is misleading, as k_{edr} must obviously be nonzero and positive. Furthermore, if χ is fixed, then k_{edr} can be determined very accurately from the data. It is therefore more meaningful to quote a range of k_{edr} based on the upper and lower estimates of χ, which results in a k_{edr} range of 1.36 × 10^{-55} $cm^{9.78}$ s^{-1} to 8.35 × 10^{-49} $cm^{8.64}$ s^{-1} for the n_{peak}−k_{obs} plot. Fortunately, what is most interesting here is the value of $k_{rg}[I^-]$, which can be determined reliably from the data. Since the difference in $k_{rg}[I^-]$ determined from the two plots in Figure 2 is negligibly small (within error estimates), the value derived from the n_{peak}−k_{obs} plot was chosen to calculate k_{rg} and η_{rg}, but identical conclusions can be drawn if the other value is used. Dividing $k_{rg}[I^-]$ by the added $[I^-]$ yields (1.24 ± 0.03) × 10^4 M^{-1} s^{-1} for k_{rg}, which is about 62 times smaller than a recently reported value for the N719 dye in the same solvent.[9] The difference is probably ascribable to the presence of bulky nonyl chains on the Z907 molecule, which may sterically hinder the approach of I^-.

Figure 3 shows η_{rg} calculated from the TA results as a function of either n_{bg} or n_{peak}. The difference between these quantities is unimportant for the present discussion, and its significance will be explained shortly. It is evident that regeneration is almost 100% efficient at low n_{tot}, but that it becomes significantly less efficient as n_{tot} increases, as predicted by eq 1. The conclusion that regeneration is 100% efficient at the lowest n_{tot} can also be drawn using data for the inert cell to estimate $k_{edr}n_{tot}^{\chi}$, although, as we will explain shortly, we are not confident that this approach is generally valid. To further confirm the observations from TA, η_{rg} was also determined from UV−vis, differential IPCE, and IS measurements, as described in our previous work.[11,27] Briefly, the method is based on the following equation:

$$\eta_{IPCE} = \eta_{lh}\eta_{inj}\eta_{rg}\eta_{col} \quad (7)$$

where η_{IPCE} is the differential IPCE measured with the cell biased to the open circuit, η_{lh} is the light harvesting efficiency, η_{inj} is the electron injection efficiency, η_{rg} is the dye regeneration efficiency (refer to eq 1), and η_{col} is the charge collection efficiency (calculated from IS fitting results and optical measurements using expressions that are given elsewhere).[28,29] Note that, for these specific measurement conditions (differential IPCE at the open-circuit voltage), η_{rg} is mathematically identical to the large-amplitude (or integral) regeneration efficiency given by eq 1, despite this being a form of differential measurement, and η_{col} does not account for the majority of collection losses due to EDR, aside from a slight decrease in the electron lifetime. Both of these facts may seem quite unintuitive but are readily proven by linearization of the electron continuity equation for these conditions. With the assumption that η_{rg} is unity at the lowest measured n_{tot}, which is expected from eq 1 and validated by the TA measurements, η_{rg} can be determined at each n_{tot} from the measured

IPCE data. Results of this analysis are also plotted *versus* n_{tot} in Figure 3.

In order to make a fair comparison between η_{rg} values determined by the two methods, we must consider the effect of perturbing n_{tot} in the TA measurements. Two points must be considered in this regard: (i) the size of the perturbation and (ii) the fact that the perturbation in n_{tot} is exclusively positive; that is, the light intensity incident on the cell is only ever increased above its background level by the laser pulse, never decreased. This contrasts with the differential IPCE measurements where the perturbation of the light intensity is substantially smaller and is both positive and negative, so that the average intensity, and thus the average n_{tot}, is unaffected. A similar argument can be made about the perturbation used in the IS measurements that were used to determine $\eta_{col.}$ It follows that n_{tot} estimated from integration of C_μ is the appropriate independent-variable against which to plot η_{rg} determined from IPCE/IS, but that the average n_{tot} during the TA measurements must be somewhat larger. To quantify this effect, the initial change in n_{tot} induced by the laser pulse was estimated from the peak of V_{oc} transients monitored simultaneously with the TA, assuming a constant C_μ that was determined from IS for each background condition. The resulting initial changes in n_{tot} were almost independent of background V_{oc}, as would be expected for a constant laser pulse energy and injection efficiency, indicating that this method of estimation is reliable. The approach is also in good agreement with estimates based on the change in cell transmission at 980 nm, although this cannot be measured as easily as the V_{oc} transient. The average change in n_{tot} estimated in this way is 1.3×10^{17} cm^{-3}, corresponding to increases in n_{tot} of 74%, 23%, 17%, 14%, 11%, and 10% for open-circuit TA at 610, 690, 715, 736, 757, and 769 mV, respectively. Without examination of the linearity of the system with numerical simulations and/or experiments using different pulse energies, it is difficult to comment on the impact of these perturbation sizes on the decay kinetics, although it is plausible that nonlinear EDR kinetics due to time-dependent n_{tot} could contribute to the deviation of the decays from being single-exponential. Fortunately, the data are still well fitted with the stretched exponential model (eq 3 and eq 4), and thus the steady-state η_{rg} can still be determined from the weighted-average D^+ lifetimes. However, correctly defining an "effective" n_{tot} for the TA measurements at which a fair comparison between η_{rg} estimates can be made is problematic at the lower end of the n_{tot} range. However, the upper and lower bounds for n_{tot} are obviously n_{peak} and n_{bg}, respectively. Since it is nontrivial to define an adequate "effective" n_{tot} against which to plot the TA-derived η_{rg}, two plots of η_{rg} are shown in Figure 3, one *versus* n_{bg} and the other *versus* n_{peak}.

As can be seen from Figure 3, η_{rg} calculated from the IPCE/IS method is in reasonable agreement with that calculated from the TA results for either estimate of n_{tot} and in excellent agreement when plotted *versus* n_{peak}. Moreover, the plot can be well fitted by eq 1 with the assumption of constant $k_{rg}[I^-]$, as shown by the line in Figure 3. The resultant EDR reaction order χ from the IPCE/IS method is 3.6 $\pm$ 0.1, while it was previously estimated to be 3.07 $\pm$ 0.19 or 2.54 $\pm$ 0.25 by fitting the $n_{tot}-k_{obs}$ data derived from TA measurements. The origin of the small discrepancies is unknown, but they may arise from issues related to the time dependence of n_{tot} in the TA measurements. A more accurate treatment would involve fitting the TA decays with a numerical model that explicitly considers the time dependence of n_{tot} when the laser-induced electron concentration is not negligible compared with the background concentration (performing experiments with lower pulse energies is difficult due to a degraded signal-to-noise ratio). In any case, the close coincidence between η_{rg} plots derived from transient and steady-state methods supports the simple model used here and confirms that the main cause of the decrease in IPCE with increasing n_{tot}/V_{oc} is incomplete dye regeneration, as we previously suggested on the basis of less direct measurements.[11]

Dependence of Electron Concentration on Incident Photon Flux in Regular and Inert Cells. In most published work where dye regeneration kinetics are investigated, the EDR rate "constant" (often derived from a half-time) for the D^+ decay ($k_{edr}n_{tot}^{\chi}$ in our notation) is estimated from the TA decay of cells/films in the absence of the redox couple, but with otherwise identical experimental conditions. A possible problem with this approach is that, due to the different removal pathways for D^+ and e^- available with and without the redox mediator, the "average" n_{tot} (which technically is time-dependent unless a small-perturbation measurement is made with a bright background light) during the TA decay is not the same in the two kinds of cells, even with identical laser pulse energy, which could lead to estimates of $k_{edr}n_{tot}^{\chi}$ that are not relevant to cells with a redox-active electrolyte. This problem will be more severe if (i) the bandwidth of the probe beam is not limited to wavelengths where D does not absorb, (ii) too large a laser pulse energy is used, (iii) too fast a repetition rate is used so that the laser-induced electron and D^+ concentrations do not fully decay to zero within one repetition period, and (iv) a deliberately added background light is used (*e.g.*, 1 sun) but the same laser intensity is used for regular and inert cells. It is also worth pointing out that if a background light is not used, then the decay of D^+ and e^- in the inert cells should be "bimolecular" (although the overall reaction order need not be 2 due to the likely nonunity order in n_{tot}); thus the pseudo-first-order approximation that is implicitly made in most data analysis is invalid.

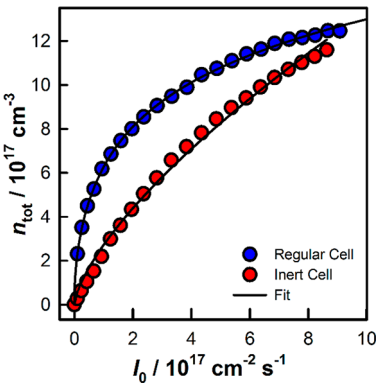

Figure 4. Steady-state dependence of TiO_2 electron concentration (n_{tot}; determined from the cell transmission at 980 nm) on incident photon flux (I_0; λ = 627 nm). The black lines are fits of eq 8 and eq 9 to the regular and inert cell data, respectively.

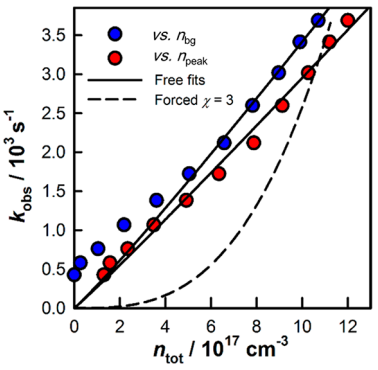

Figure 5. Dependence of the observed rate constant (k_{obs}) on TiO_2 electron concentration (n_{tot}) obtained from transient absorption measurements made on inert cells with a redox-inactive electrolyte solution. The solid lines are free fits of eq 10 to the data, from which the electron−dye recombination reaction order (χ) in n_{tot} can be estimated. Also shown is a fit with χ fixed to 3, approximately the value obtained from various different measurements for regular cells with a redox-active electrolyte solution.

In order to examine some of these points in more detail, n_{tot} in regular and inert cells was compared under various background light intensities by steady-state transmission measurements at 980 nm, where only e^- absorbs. The results are shown in Figure 4, where n_{tot} is plotted *versus* the incident photon flux (I_0; λ = 627 nm) for regular and inert cells. Clearly, n_{tot} is quite different in the two kinds of cells at any given I_0. This demonstrates that n_{tot} should be carefully measured in regular and inert cells. To further examine the differences between regular and inert cells, the $n_{tot}-I_0$ plots were fitted to extract the reaction orders in n_{tot} for EDR and, for the regular cell, EER. For regular cells with spatially uniform generation (weakly absorbed light) at steady state we can write[11,27]

$$I_0\eta_{lh}\eta_{inj}/d = k'_{eer}n_{tot}^{\gamma} + \frac{k'_{eer}k_{edr}}{k_{rg}[I^-]}n_{tot}^{\gamma+\chi} \quad (8)$$

where k'_{eer} is the rate constant for EER and γ is the order in n_{tot}. For inert cells, since e^- can only recombine with D^+ and their concentrations must be equal, it can easily be shown that

$$I_0\eta_{lh}\eta_{inj}/d = k_{edr}n_{tot}^{\chi+1} \quad (9)$$

The regular cell data are fitted well by eq 8, and it is worth noting that the fit quality is improved by a statistically significant amount compared to a single power law fit. The fit of eq 9 to the inert cell data is less satisfactory. Obviously, the fit might be improved if eq 8 was used instead, but there is no physical basis for doing so. The resultant χ from the fit to the regular cell is 3.1 ± 0.4, which is very close to χ derived from TA measurements if $n_{tot} = n_{peak}$ is assumed (3.07 ± 0.19) and just within error estimates of that derived from IPCE/IS (3.6 ± 0.1). The approximate agreement between these three independent approaches, one dynamic and two steady-state, validates the model used here and increases confidence in the range of values that χ can take. On the other hand, χ for the inert cell is only 0.44 ± 0.01, very far from that obtained for the regular cells. This large discrepancy in EDR reaction order suggests that there is some fundamental difference in the EDR recombination mechanism between regular and inert cells. It follows that, at least for the cells studied here, the common practice of using the EDR rate constant obtained from inert cells to calculate $k_{rg}[I^-]$ or η_{rg} in regular cells is incorrect, even if care is taken to make small-perturbation measurements at matched n_{tot}.

Dependence of Electron−Dye Recombination Rate Constant on Electron Concentration in Inert Cells. To further investigate recombination kinetics in inert cells and the validity of using the EDR rate constant obtained from these cells to calculate $k_{rg}[I^-]$ or η_{rg} for regular cells, TA decays at 830 nm were also measured for inert cells over a range of background light intensities. The TA decays were fitted with a single stretched exponential, and k_{obs} was calculated as before. The electron concentration in the cells was estimated from the steady-state 980 nm OD change relative to the dark. The dependence of k_{obs} on n_{tot} is shown in Figure 5.

Provided the background illumination is strong enough that the TA measurement can be considered to be in the small-perturbation regime, the dependence of k_{obs} on n_{tot} for inert cells is given by

$$k_{obs} = (\chi+1)k_{edr}n_{tot}^{\chi} \quad (10)$$

However, for measurements with little or no background light, the laser-induced e^- and D^+ concentrations are significant and eq 10 need not be obeyed. If we take n_{tot} to be equal to n_{bg} and fit eq 10 to only the top five data points (where the laser-induced e^- concentration is less than ~20% of n_{tot}), a value of 1.14 ± 0.02 is obtained for χ, which, as found in the steady-state measurements, is much lower than that obtained for the regular cells. A similarly low value of 1.04 ± 0.05 for χ is obtained if $n_{tot} = n_{peak}$ is assumed, and the

entire data set is fitted instead. These values are also quite different from χ derived from steady-state measurements made on the same cell (0.44 ± 0.01), although still in better agreement with this than with any of the regular cell measurements. To help appreciate the discrepancy in χ between regular and inert cells more clearly, the data were also fitted with χ fixed to 3 (approximately the value found for the regular cells by various techniques), which, as can be seen from Figure 5, results in a very poor fit. These findings provide further evidence that the practice of using TA measurements made with redox-inactive electrolyte solutions in the calculation of regeneration rate constants or efficiencies is questionable.

We have not yet established the reason for χ in inert cells being so different from that in regular cells. It may be that some specific interaction between either half of the redox mediator (or the salt added to substitute it in the inert cell) and the dye and/or TiO_2 alters the EDR mechanism, *e.g.*, by shifting the TiO_2 conduction band energy relative to the dye energy levels, which could alter the apparent reaction order if surface states are involved in recombination.[30−33] It should also be noted that in the absence of the redox mediator the TiO_2 particles are not expected to be depleted at equilibrium in the dark. This means that the actual electron concentration in the particles, and therefore also the energies of occupied states, may not be the same in regular and inert cells for the same n_{tot}, although this effect would be less important for photoinduced electron concentrations that are much greater than the (unknown) doping density of the TiO_2 particles. However, it seems unlikely that either of these explanations could give rise to such a large difference in reaction order. Another possibility is that the presumably very high D^+ concentration in the inert cell (in principle equal to n_{tot} if no other pathway for removal of D^+ exists) compared to the regular cell leads to a change in the reaction order in $[D^+]$, although we have no direct evidence to support this.

Regeneration Efficiency under Working Conditions. To estimate the regeneration efficiency under operating conditions, TA at 830 nm was measured with cells biased to the MPP on the $j-V$ curve under background illumination that produced about one-third of the 1 sun j_{sc}. The TA decay was then fitted as before to obtain k_{obs}, from which a value of ~90% for η_{rg} was calculated using the value of $k_{rg}[I^-]$ determined in the open-circuit measurements. The perturbation in n_{tot} during the TA experiment was examined by monitoring the transmission of the cell at 980 nm and was found to be ~30% of the background n_{tot}. Similar experiments were also performed at short circuit, which produced η_{rg} values of >99%. It could be argued that using $k_{rg}[I^-]$ from the open-circuit measurements in these calculations is not appropriate due to the $[I^-]$ gradient caused by current flow at short circuit or the

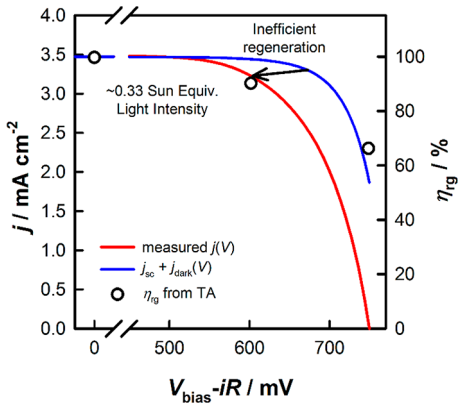

Figure 6. Measured $j-V$ characteristic (red line) for a regular cell and the $j-V$ characteristic predicted (blue line) from the sum of the short-circuit photocurrent and the dark current, as would be expected if dye regeneration was 100% efficient and no additional recombination pathways open up under illumination. Also shown is the regeneration efficiency (circles, right *y*-axis), η_{rg}, obtained from TA measurements made at short circuit, the maximum power point (MPP), and open circuit. All measurements were made under illumination (λ = 627 nm) equivalent to ~0.33 sun absorbed intensity. Note that all of the drop in current at the MPP can be ascribed to dye regeneration losses.

MPP. However, if this effect is significant, then using the open-circuit value of $k_{rg}[I^-]$ will result in overestimation of η_{rg}, and thus our estimate can be viewed as an upper limit for η_{rg}. Furthermore, taking the diffusion coefficient of I^- in 3-methoxypropionitrile solution to be ~4.5×10^{-6} cm^2 s^{-1},[17] we estimate that only a 1.5% decrease in $[I^-]$ at the substrate is required to support the photocurrent. Even if the diffusion coefficient is reduced by a factor of 3 throughout the entire 25 μm thick electrolyte layer, which should overcorrect for constrictivity and tortuosity effects due to diffusion in the TiO_2 pores,[10,34,35] a maximum $[I^-]$ depletion of only 4.5% is calculated, which will have a very minor effect on our η_{rg} calculations.

To correlate η_{rg} obtained from TA with the $j-V$ characteristic, the measured $j-V$ was corrected for *iR* drop across the series resistance and then compared with the simulated $j-V$ obtained by adding j_{sc} to the measured dark $j-V$, also corrected for *iR* drop. As can be seen in Figure 6, the current loss at the MPP compared to j_{sc} is ~8%, which is remarkably close to the ~10% regeneration loss predicted by the TA measurements. This is an extremely important finding, as it implies that the efficiency of these DSCs could be improved if regeneration could be made faster, despite the fact that it appears perfect at short circuit. Note that conventional IPCE measurements, the linearity of the j_{sc}-light intensity characteristics, and TA measurements made with weak laser pulses without bias/background light would all be incapable of identifying that the efficiency of this cell was limited by inefficient regeneration. On first sight, the potential improvement in efficiency seems to be fairly small, as the regeneration efficiency at the MPP is still relatively high. However,

it must be realized that V_{oc} and fill factor (FF) are also partly determined by the voltage dependence of regeneration. As shown in Figure 6, both V_{oc} and FF of the simulated $j-V$ assuming perfect dye regeneration are enhanced, while the increase in j at the MPP is actually rather insignificant. Overall, a 14% improvement in PCE (now limited by the dark current curve) would be achieved if regeneration could be made more efficient.

CONCLUSION

Dye regeneration and recombination kinetics in complete DSCs were characterized by TA, differential IPCE, and IS measurements over a range of background light intensities at open circuit. TA measurements were also performed at short circuit and at the MPP. By combining the results of these experiments, the dependence of η_{rg} on n_{tot} in a complete DSC has been unambiguously demonstrated for the first time, with good agreement between TA measurements and steady-state IPCE measurements being found. In principle, the protocol established here can be applied to other DSC systems, such as DSCs employing Co-complex mediators and solid-state DSCs. More importantly, a ~10% loss in η_{rg} was measured at the MPP for these cells, indicating that inefficient regeneration limits their efficiency. It is estimated that a 14% improvement in PCE for these cells could be achieved if regeneration was 100% efficient under all conditions, so that the shape of the $j-V$ characteristic was determined only by the dark current. We predict that the PCE of other robust DSCs could be improved further by accelerating dye regeneration kinetics, even if standard tests such as conventional IPCE, the linearity of j_{sc} *versus* light intensity, and *ex situ* TA measurements (without carefully controlled electron concentration) all indicate perfect regeneration. Finally, TA measurements made as a function of n_{tot}, and measurements of n_{tot} as a function of light intensity, reveal that redox-inactive "inert" cells are probably not suitable for the determination of the EDR rate constant in regular cells, as these cells exhibit a different EDR order in n_{tot}. It is therefore recommended that $k_{rg}[I^-]$ be determined instead by making measurements on regular cells over a range of n_{tot}, including very low n_{tot}, or by varying $[I^-]$, or ideally both.

METHODS

Fabrication of Dye-Sensitized Solar Cells. The DSCs used in this work were fabricated following a protocol described in detail elsewhere,[36] and only pertinent details will be given here. Mesoporous TiO_2 layers were prepared by screen printing a commercially available TiO_2 paste (90-T, Dyesol). The thickness of the resultant layers was determined to be *ca.* 5.4 μm using a surface profiler (AlphaStep IQ, KLA-Tencor). TiO_2 electrodes were sensitized by immersion in a 0.15 mM solution of *cis*-diisothiocyanato(2,2′-bipyridyl-4,4′-dicarboxylic acid)-(2,2′-bipyridyl-4,4′-dinonyl)ruthenium(II) (Z907) in 1:1 (v/v) acetonitrile/*tert*-butanol solution for *ca.* 16 h. The electrolyte solution consisted of 1 M propylmethylimidazolium iodide (PMII), 0.15 M I_2, 0.5 M *N*-methylbenzimidazole, and 0.1 M guanidinium thiocyanate in 3-methoxypropionitrile.[24] Cells were also constructed with a redox-inactive "inert" electrolyte solution that was identical in composition except that PMII and I_2 were replaced with 1 M 1-ethyl-3-methylimidazolium bis(trifluoromethylsulfonyl)-imide, in order to maintain the same ionic strength as the regular electrolyte. All measurements presented herein were performed on a pair of nominally identical cells to check reproducibility. The average PCE of these cells was 4.55% (j_{sc} = 10.1 mA cm^{-2}, V_{oc} = 763 mV, FF = 59.2%) under simulated AM1.5G 100 mW cm^{-2} illumination. The relatively low cell efficiency compared with literature reports for similar electrolyte compositions is mainly due to the thin TiO_2 layer thickness and lack of a light scattering layer, both of which are required to facilitate accurate TA measurements.

UV–Vis and $j-V$ Measurements. The absorbance of FTO substrates and bare or dye-sensitized TiO_2 films filled with electrolyte was measured with a UV–vis–NIR spectrometer (SolidSpec-3700, Shimadzu) in direct transmission mode. Current–voltage characteristics were determined under AM 1.5 illumination provided by a Newport class A solar simulator. A shallow mask slightly larger than the electrode area was used, and the active cell area was taken to be the TiO_2 film area of 0.283 cm^2. All other parts of the cell were carefully masked to avoid light piping to the active area. All cells were stabilized in the dark at room temperature for 3 days before testing and were preilluminated with AM1.5 illumination for 30 s before the 70 s $j-V$ scan.

Impedance Spectroscopy and Differential Incident Photon-to-Current Efficiency Measurements. IS measurements were performed using a potentiostat equipped with a frequency response analyzer (Autolab PGSTAT 302N/FRA2, Ecochemie). Cells were biased to the open-circuit photovoltage induced by illumination from a high-power red LED (λ = 627 nm, Luxeon). Different light intensities and photovoltages were achieved by using neutral density filters mounted in an automated filter wheel system (Newport). Under the highest intensity *ca.* 40% of the photocurrent under 1 sun illumination was delivered by the cells. IPCE measurements with cells biased near open circuit (referred to as differential IPCE) were made immediately after IS measurements by modulating the amplitude of the LED driving current ± 4% and recording the change in cell current. The change in photon flux caused by modulation of the LED current was measured using a calibrated photodiode (FDS100, Thorlabs). Current–voltage characteristics at each illumination intensity and in the dark were also recorded following the IS and IPCE measurements.

Transient Absorption. TA measurements were performed using a home-built system. Samples were excited with laser pulses provided by a Nd:YAG Q-switched laser (Continuum Minilite II, 532 nm, 5 ns pulse width, 5 Hz repetition rate, 30 μJ cm^{-2} per pulse, nominal beam diameter 9 mm after 3× beam expander). Two near-infrared LEDs with emission spectra centered at 850 and 970 nm (M850L2, M970L2, *ca.* 100 nm emission width, Thorlabs) were used to provide the probe light. LED light was selected due to its superior stability on millisecond to second time scales compared with other available light sources. Laser pulses and probe light were combined using a dichroic mirror to produce a collinear beam that was normally incident on the cell under test. A photodiode detector (Thorlabs FDS100, 10 ns rise time) was positioned behind the cell to record the intensity of the transmitted light. Either an 830 nm or a 980 nm bandpass filter (10 nm pass band) and a 532 nm notch filter were mounted in front of the photodiode to reject stray light. The photodiode was operated at 10 V reverse bias to improve response time, and the photocurrent was measured using a current amplifier (FEMTO DHPCA-100, 80 MHz bandwidth) and an oscilloscope (Tektronix DPO2022B, 200 MHz bandwidth) controlled by a

computer using Labview. A photodiode with an integrated current amplifier (PDA36A, Thorlabs) was used as a trigger. The same 627 nm LED used for IS measurements was used to provide various levels of background light during the TA measurements. During measurements made at open circuit, the transient photovoltage of the cells was monitored simultaneously on the other channel of the oscilloscope. Kinetic traces were averaged 728 times, and data were processed in Wolfram Mathematica 8. For measurements made at short circuit or the MPP, a Keithley SourceMeter was used to provide an electrical bias to the cell. In all these measurements the j_{sc} produced by the background light was about one-third of the 1 sun j_{sc}. During all TA measurements, the front surface of the cell was covered with the same shallow mask used for $j-V$ and IS measurements, while the rear surface was covered by a mask slightly smaller than the active area. With this configuration, all parts of the active layer are excited by the laser pulse, probe, and background light, but stray probe light (*i.e.*, not passing through the TiO_2 layer) cannot reach the photodiode detector located behind the sample.

Steady-State Transmission. The steady-state transmission of cells at 980 nm under various background illumination intensities and external bias voltages was recorded with the same photodiode detector used for TA measurements. To enhance the signal-to-noise ratio, the probe light was modulated at 10 kHz and the signal was detected using a lock-in amplifier (SR830, Stanford Research Systems).

Conflict of Interest: The authors declare no competing financial interest.

Acknowledgment. This research was supported by the National Research Foundation of Singapore under its Competitive Research Program (CRP Award No. NRF-CRP4-2008-03).

Supporting Information Available: Comparison of fitting results for the electron decay monitored at 830 and 980 nm. This material is available free of charge *via* the Internet at http://pubs.acs.org.

REFERENCES AND NOTES

1. Yella, A.; Lee, H.-W.; Tsao, H. N.; Yi, C.; Chandiran, A. K.; Nazeeruddin, M. K.; Diau, E. W.-G.; Yeh, C.-Y.; Zakeeruddin, S. M.; Grätzel, M. Porphyrin-Sensitized Solar Cells with Cobalt (II/III)-Based Redox Electrolyte Exceed 12% Efficiency. *Science* **2011**, *334*, 629–634.
2. Oregan, B.; Grätzel, M. A Low-Cost, High-Efficiency Solar-Cell Based on Dye-Sensitized Colloidal TiO_2 Films. *Nature* **1991**, *353*, 737–740.
3. Grätzel, M. Photoelectrochemical Cells. *Nature* **2001**, *414*, 338–344.
4. O'Regan, B.; Moser, J.; Anderson, M.; Grätzel, M. Vectorial Electron Injection into Transparent Semiconductor Membranes and Electric Field Effects on the Dynamics of Light-Induced Charge Separation. *J. Phys. Chem.* **1990**, *94*, 8720–8726.
5. Nazeeruddin, M. K.; Kay, A.; Rodicio, I.; Humphrybaker, R.; Muller, E.; Liska, P.; Vlachopoulos, N.; Gratzel, M. Conversion of Light to Electricty by *cis*-X_2-bis(2,2′-bipyridyl-4,4′-dicarboxylate)ruthenium(II) Charge-Transfer Sensitizers (X = Cl^-, Br^-, I^-, CN^-, and SCN^-) on Nanocrystalline TiO_2 Electrodes. *J. Am. Chem. Soc.* **1993**, *115*, 6382–6390.
6. Hagfeldt, A.; Grätzel, M. Light-Induced Redox Reactions in Nanocrystalline Systems. *Chem. Rev.* **1995**, *95*, 49–68.
7. Huang, S. Y.; Schlichthorl, G.; Nozik, A. J.; Grätzel, M.; Frank, A. J. Charge Recombination in Dye-Sensitized Nanocrystalline TiO_2 Solar Cells. *J. Phys. Chem. B* **1997**, *101*, 2576–2582.
8. Haque, S. A.; Tachibana, Y.; Willis, R. L.; Moser, J. E.; Grätzel, M.; Klug, D. R.; Durrant, J. R. Parameters Influencing Charge Recombination Kinetics in Dye-Sensitized Nanocrystalline Titanium Dioxide Films. *J. Phys. Chem. B* **2000**, *104*, 538–547.
9. Anderson, A. Y.; Barnes, P. R. F.; Durrant, J. R.; O'Regan, B. C. Quantifying Regeneration in Dye-Sensitized Solar Cells. *J. Phys. Chem. C* **2011**, *115*, 2439–2447.
10. Barnes, P. R. F.; Anderson, A. Y.; Durrant, J. R.; O'Regan, B. C. Simulation and Measurement of Complete Dye Sensitised Solar Cells: Including the Influence of Trapping, Electrolyte, Oxidised Dyes and Light Intensity on Steady State and Transient Device Behaviour. *Phys. Chem. Chem. Phys.* **2011**, *13*, 5798–5816.
11. Jennings, J. R.; Liu, Y.; Wang, Q. Efficiency Limitations in Dye-Sensitized Solar Cells Caused by Inefficient Sensitizer Regeneration. *J. Phys. Chem. C* **2011**, *115*, 15109–15120.
12. Boschloo, G.; Hagfeldt, A. Characteristics of the Iodide/Triiodide Redox Mediator in Dye-Sensitized Solar Cells. *Acc. Chem. Res.* **2009**, *42*, 1819–1826.
13. Pelet, S.; Moser, J. E.; Grätzel, M. Cooperative Effect of Adsorbed Cations and Iodide on the Interception of Back Electron Transfer in the Dye Sensitization of Nanocrystalline TiO_2. *J. Phys. Chem. B* **2000**, *104*, 1791–1795.
14. Clifford, J. N.; Palomares, E.; Nazeeruddin, M. K.; Grätzel, M.; Durrant, J. R. Dye Dependent Regeneration Dynamics in Dye Sensitized Nanocrystalline Solar Cells: Evidence for the Formation of a Ruthenium Bipyridyl Cation/Iodide Intermediate. *J. Phys. Chem. C* **2007**, *111*, 6561–6567.
15. Alebbi, M.; Bignozzi, C. A.; Heimer, T. A.; Hasselmann, G. M.; Meyer, G. J. The Limiting Role of Iodide Oxidation in cis-$Os(dcb)_2(CN)_2/TiO_2$ Photoelectrochemical Cells. *J. Phys. Chem. B* **1998**, *102*, 7577–7581.
16. Martiniani, S.; Anderson, A. Y.; Law, C.; O'Regan, B. C.; Barolo, C. New Insight into the Regeneration Kinetics of Organic Dye Sensitised Solar Cells. *Chem. Commun. (Cambridge, U. K.)* **2012**, *48*, 2406–2408.
17. Zhang, Z.; Ito, S.; Moser, J. E.; Zakeeruddin, S. M.; Grätzel, M. Influence of Iodide Concentration on the Efficiency and Stability of Dye-Sensitized Solar Cell Containing Non-Volatile Electrolyte. *ChemPhysChem* **2009**, *10*, 1834–1838.
18. Feldt, S. M.; Wang, G.; Boschloo, G.; Hagfeldt, A. Effects of Driving Forces for Recombination and Regeneration on the Photovoltaic Performance of Dye-Sensitized Solar Cells Using Cobalt Polypyridine Redox Couples. *J. Phys. Chem. C* **2011**, *115*, 21500–21507.
19. Daeneke, T.; Mozer, A. J.; Kwon, T.-H.; Duffy, N. W.; Holmes, A. B.; Bach, U.; Spiccia, L. Dye Regeneration and Charge Recombination in Dye-Sensitized Solar Cells with Ferrocene Derivatives as Redox Mediators. *Energy Environ. Sci.* **2012**, *5*, 7090–7099.
20. Daeneke, T.; Mozer, A. J.; Uemura, Y.; Makuta, S.; Fekete, M.; Tachibana, Y.; Koumura, N.; Bach, U.; Spiccia, L. Dye Regeneration Kinetics in Dye-Sensitized Solar Cells. *J. Am. Chem. Soc.* **2012**, *134*, 16925–16928.
21. Peter, L. M. Dye-Sensitized Nanocrystalline Solar Cells. *Phys. Chem. Chem. Phys.* **2007**, *9*, 2630–2642.
22. Peter, L. M. Characterization and Modeling of Dye-Sensitized Solar Cells. *J. Phys. Chem. C* **2007**, *111*, 6601–6612.
23. Haque, S. A.; Tachibana, Y.; Klug, D. R.; Durrant, J. R. Charge Recombination Kinetics in Dye-Sensitized Nanocrystalline Titanium Dioxide Films under Externally Applied Bias. *J. Phys. Chem. B* **1998**, *102*, 1745–1749.
24. Chen, C.-Y.; Pootrakulchote, N.; Hung, T.-H.; Tan, C.-J.; Tsai, H.-H.; Zakeeruddin, S. M.; Wu, C.-G.; Grätzel, M. Ruthenium Sensitizer with Thienothiophene-Linked Carbazole Antennas in Conjunction with Liquid Electrolytes for Dye-Sensitized Solar Cells. *J. Phys. Chem. C* **2011**, *115*, 20043–20050.
25. Shi, D.; Pootrakulchote, N.; Li, R.; Guo, J.; Wang, Y.; Zakeeruddin, S. M.; Grätzel, M.; Wang, P. New Efficiency Records for Stable Dye-Sensitized Solar Cells with Low-Volatility and Ionic Liquid Electrolytes. *J. Phys. Chem. C* **2008**, *112*, 17046–17050.
26. Wang, Q.; Zakeeruddin, S. M.; Nazeeruddin, M. K.; Humphry-Baker, R.; Grätzel, M. Molecular Wiring of Nanocrystals: NCS-Enhanced Cross-Surface Charge Transfer in Self-Assembled Ru-Complex Monolayer on Mesoscopic Oxide Films. *J. Am. Chem. Soc.* **2006**, *128*, 4446–4452.
27. Jennings, J. R.; Li, F.; Wang, Q. Reliable Determination of Electron Diffusion Length and Charge Separation Efficiency in Dye-Sensitized Solar Cells. *J. Phys. Chem. C* **2010**, *114*, 14665–14674.

28. Halme, J.; Boschloo, G.; Hagfeldt, A.; Lund, P. Spectral Characteristics of Light Harvesting, Electron Injection, and Steady-State Charge Collection in Pressed TiO_2 Dye Solar Cells. *J. Phys. Chem. C* **2008**, *112*, 5623–5637.
29. Bisquert, J. Theory of the Impedance of Electron Diffusion and Recombination in a Thin Layer. *J. Phys. Chem. B* **2002**, *106*, 325–333.
30. Salvador, P.; Hidalgo, M. G.; Zaban, A.; Bisquert, J. Illumination Intensity Dependence of the Photovoltage in Nanostructured TiO_2 Dye-Sensitized Solar Cells. *J. Phys. Chem. B* **2005**, *109*, 15915–15926.
31. Jennings, J. R.; Wang, Q. Influence of Lithium Ion Concentration on Electron Injection, Transport, and Recombination in Dye-Sensitized Solar Cells. *J. Phys. Chem. C* **2010**, *114*, 1715–1724.
32. Liu, Y.; Jennings, J. R.; Zakeeruddin, S. M.; Grätzel, M.; Wang, Q. Heterogeneous Electron Transfer from Dye-Sensitized Nanocrystalline TiO_2 to $[Co(bpy)_3]^{3+}$: Insights Gained from Impedance Spectroscopy. *J. Am. Chem. Soc.* **2013**, *135*, 3939–3952.
33. Ansari-Rad, M.; Anta, J. A.; Bisquert, J. Interpretation of Diffusion and Recombination in Nanostructured and Energy-Disordered Materials by Stochastic Quasiequilibrium Simulation. *J. Phys. Chem. C* **2013**, *117* 16275−16289.
34. Papageorgiou, N.; Barbe, C.; Grätzel, M. Morphology and Adsorbate Dependence of Ionic Transport in Dye Sensitized Mesoporous TiO_2 Films. *J. Phys. Chem. B* **1998**, *102*, 4156–4164.
35. Kron, G.; Egerter, T.; Werner, J. H.; Rau, U. Electronic Transport in Dye-Sensitized Nanoporous TiO_2 Solar Cells − Comparison of Electrolyte and Solid-State Devices. *J. Phys. Chem. B* **2003**, *107*, 3556–3564.
36. Jennings, J. R.; Liu, Y.; Safari-Alamuti, F.; Wang, Q. Dependence of Dye-Sensitized Solar Cell Impedance on Photoelectrode Thickness. *J. Phys. Chem. C* **2011**, *116*, 1556–1562.